



The adsorption of HCl on volcanic ash

Xochilt Gutiérrez, Federica Schiavi, Hans Keppler

► To cite this version:

Xochilt Gutiérrez, Federica Schiavi, Hans Keppler. The adsorption of HCl on volcanic ash. Earth and Planetary Science Letters, 2016, 438, pp.66-74. 10.1016/j.epsl.2016.01.019 . hal-02404351

HAL Id: hal-02404351

<https://uca.hal.science/hal-02404351>

Submitted on 11 Dec 2019

HAL is a multi-disciplinary open access archive for the deposit and dissemination of scientific research documents, whether they are published or not. The documents may come from teaching and research institutions in France or abroad, or from public or private research centers.

L'archive ouverte pluridisciplinaire **HAL**, est destinée au dépôt et à la diffusion de documents scientifiques de niveau recherche, publiés ou non, émanant des établissements d'enseignement et de recherche français ou étrangers, des laboratoires publics ou privés.

The adsorption of HCl on volcanic ash

Xochilt Gutierrez, Federica Schiavi, and Hans Keppler*

Bayerisches Geoinstitut, Universität Bayreuth, 95440 Bayreuth, Germany

*Corresponding author: hans.keppler@uni-bayreuth.de

Abstract. Understanding the interaction between volcanic gases and ash is important to derive gas compositions from ash leachates and to constrain the environmental impact of eruptions. Volcanic HCl could potentially damage the ozone layer, but it is unclear what fraction of HCl actually reaches the stratosphere. The adsorption of HCl on volcanic ash was therefore studied from -76 to + 150 °C to simulate the behavior of HCl in the dilute parts of a volcanic plume. Finely ground synthetic glasses of andesitic, dacitic, and rhyolitic composition as well as a natural obsidian from Vulcano (Italy) served as proxies for fresh natural ash. HCl adsorption is an irreversible process and appears to increase with the total alkali content of the glass. Adsorption kinetics follow a first order law with rate constants of $2.13 \cdot 10^{-6} \text{ s}^{-1}$ to $1.80 \cdot 10^{-4} \text{ s}^{-1}$ in the temperature range investigated. For dacitic composition, the temperature and pressure dependence of adsorption can be described by the equation $\ln c = 1.26 + 0.27 \ln p - 715.3/T$, where c is the surface concentration of adsorbed HCl in mg/m^2 , T is temperature in Kelvin, and p is the partial pressure of HCl in mbar. A comparison of this model with a large data set for the composition of volcanic ash suggests that adsorption of HCl from the gas phase at relatively low temperatures can quantitatively account for the majority of the observed Cl concentrations. The model implies that adsorption of HCl on ash increases with temperature, probably because of

the increasing number of accessible adsorption sites. This temperature dependence is opposite to that observed for SO₂, so that HCl and SO₂ are fractionated by the adsorption process and the fractionation factor changes by four orders of magnitude over a temperature range of 250 K. The assumption of equal adsorption of different species is therefore not appropriate for deriving volcanic gas compositions from analyses of adsorbates on ash. However, with the experimental data provided here, the gas compositions in equilibrium with the ash surfaces can be calculated. In particular, for dacitic composition, the molar ratio of S/Cl adsorbed to the ash surface is related to the molar S/Cl ratio in the gas phase according to the equation $\ln (S/Cl)_{\text{adsorbed}} = 2855 T^{-1} + 0.28 \ln (S/Cl)_{\text{gas}} - 11.14$. Our data also show that adsorption on ash will significantly reduce the fraction of HCl reaching the stratosphere, only if the initial HCl content in the volcanic gas is low (< 1 mole %). For higher initial HCl concentrations, adsorption on ash has only a minor effect. While HCl scavenging by hydrometeors may remove a considerable fraction of HCl from the eruption column, recent models suggest that this process is much less efficient than previously thought. Our experimental data therefore support the idea that the HCl loading from major explosive eruptions may indeed cause severe depletions of stratospheric ozone.

Keywords: Adsorption, ash, hydrogen chloride, volcanic gases, ozone

1. Introduction

The short-term climatic impact of volcanic eruptions is mostly due to the interaction of sulfur and halogen species in volcanic gases with the atmosphere. The surface cooling observed after major explosive eruptions is caused by the injection of sulfur dioxide into the stratosphere, where it is photochemically oxidized to sulfate aerosols.

51 These aerosols backscatter sunlight and may remain in the stratosphere for months or
52 even years (e.g. McCormick et al. 1995, Robock 2000). Ozone destruction is another
53 potential effect of large explosive eruptions, but it is much less understood than the
54 surface cooling effect. Black et al. (2014) suggested that the end-Permian mass
55 extinction partially resulted from ozone depletion associated with the Siberian Trap
56 magmatism. Measurable depletions in stratospheric ozone were observed after the
57 1991 Mt. Pinatubo eruption (Brasseur and Granier 1992, Solomon et al. 1998). They
58 were attributed to the catalytic effect of sulfate aerosol surfaces, which may enhance
59 the concentration of active chlorine species involved in ozone destruction (Solomon et
60 al. 1993, Hofmann et al. 1994). However, another mechanism could be the direct
61 injection of volcanic hydrogen chloride (HCl) into the stratosphere. A study by
62 Tabazadeh and Turco (1993) suggested that this mechanism is inefficient, because
63 hydrogen chloride would be nearly completely washed out of the eruption column by
64 condensing water. More recent models of eruption plumes (Textor et al. 2003),
65 however, show that most of the water in the plume is present as solid ice, which
66 greatly reduces the efficiency of HCl scavenging. Moreover, most of the ice particles
67 are lifted upwards, so that more than 25 % of the HCl originally contained in the
68 plume may reach the stratosphere. This prediction was confirmed for the case of a
69 high-latitude eruption by direct sampling of a volcanic cloud from Hekla volcano
70 (Rose et al. 2006, Millard et al. 2006). Spectroscopic observations also suggested an
71 increase of 40 % in the total column of HCl above 12 km altitude after the 1982 El
72 Chicón eruption (Mankin and Coffey 1984, see also Woods et al. 1985), while at most
73 a slight increase in stratospheric HCl was observed after the 1991 Mt. Pinatubo
74 eruption (Mankin et al. 1992, Wallace and Livingston 1992). Kutterolf et al. (2013)
75 estimated the Cl and Br release from 14 large explosive eruptions in Nicaragua in the

last 70 00 years and concluded that most of these eruptions likely caused significant ozone destruction in the stratosphere. On the other hand, elevated HCl concentrations are only rarely detected in ice cores; this may, however, be due to the volatilization of HCl in the presence of H₂SO₄ (Wagon et al., 1999, Zdanowicz et al. 1999, Thamman et al. 2006). The limited data available may imply that the stratospheric HCl yield of eruptions varies considerably, depending on initial gas composition and on the processes occurring in the eruption column.

Hydrogen chloride (HCl) concentrations in volcanic gases typically range from < 0.05 to > 5 mole %, with most data probably in the 0.1 to 1 mole % range (Symonds et al. 1994, Fischer 2008). Relatively high HCl concentrations and HCl/SO₂ ratios are often found in arc volcanoes. Estimated annual fluxes of HCl vary widely, from 0.4 to 170 Tg/a (Symonds et al. 1988, Halmer et al. 2002). Pyle and Mather (2009) used a compilation of measured HCl/SO₂ ratios and total SO₂ fluxes to estimate the HCl flux from arc volcanoes at 4.3 ± 1 Tg/a, which is believed to dominate the global flux. However, the flux of HCl reaching the stratosphere is certainly much lower, because only large eruptions penetrate the tropopause and processes in the eruption column may deplete HCl. While the depletion by water and ice has already been investigated in some detail, little is known about the possible effect of HCl adsorption on volcanic ash (Rose 1977). Ayris et al. (2014) studied the interaction of HCl with ash under near-vent, high-temperature conditions (200 - 800 °C). Only for alkali-rich tephrite and phonolite glasses, reaction with HCl to NaCl was observed, but not for dacite and rhyolite. The very short residence time of ash at near-vent conditions during an explosive eruption may further limit the extent of adsorption at high temperature. This suggests that HCl adsorption, if it is an important process at all, must occur in the

low-temperature portion of the dilute plume. We therefore studied the adsorption of HCl on ashes of rhyolitic, dacitic, and andesitic composition from -76 to + 150 °C at variable HCl partial pressures covering the plausible conditions in a dilute volcanic plume.

2. Experimental methods

Fe-free synthetic glasses of rhyolitic, dacitic, and andesitic composition were used as proxies for fresh volcanic ash. The glasses were prepared from homogenized, stoichiometric mixtures of analytical grade SiO₂, Al(OH)₃, MgO, CaCO₃, Na₂CO₃, and K₂CO₃. After decarbonation in a platinum crucible, the charge was melted at 1600 °C for 1 hour and quenched in deionized water, yielding a clear glass with some bubbles. Microprobe analyses are given in Table 1. The glass was then dried and ground four times for seven minutes each in a planetary mill. No liquid was added to avoid adsorption on fresh surfaces. The surface area of the powders was determined with a Quantachrome instrument by measuring the BET adsorption isotherm of krypton at 77 K. To constrain the isotherm, seven data points were measured in a range of pressures ranging from 5 to 30 % of the condensation pressure of Kr. 100 – 200 mg of sample were outgassed at 200 °C for 24 hours before the measurement. The specific surfaces obtained were in the range of 1.5 – 4.9 m²/g. These numbers are quite comparable to those obtained for fine (< 100 µm) natural ash (mostly 1.1 – 2.1 m²/g for a sieved fraction < 100 µm; Demelle et al. 2005; 4.3 m²/g for phreatomagmatic ash from Eyafjallajökull; Gislason et al. 2011).

Adsorption measurements were carried out in a glass apparatus equipped with a Vacuubrand DVR 5 pressure gauge, following the procedure described by Schmauss

126 and Keppler (2014). In brief, 30 – 50 g of the sample powder were placed in a sample
127 tube and the entire system was evacuated. HCl gas was then filled into a reservoir
128 flask up to the desired pressure. Once the valve between the sample tube and the
129 reservoir was opened, an instantaneous pressure drop occurred due to the expansion
130 of the gas into the sample tube, followed by a slow decrease in pressure due to the
131 adsorption of HCl on the sample surface. From the known volumes of the system, the
132 measured pressure drop and the temperature, the amount of adsorbed HCl can be
133 calculated. All required formulae are given by Schmauss and Keppler (2014). For
134 calculating the amount of adsorbed HCl, the ideal gas law was used, which is a very
135 good approximation for HCl under the low pressures and the temperatures of interest.
136 Once the pressure in the system had stabilized, the valve between sample and gas
137 reservoir was closed and the pressure in the reservoir was increased. After opening
138 the valve again, the next point of the adsorption isotherm was measured. This
139 procedure was repeated until the pressure in the system reached nearly one bar.
140 Desorption experiments started from close to one bar by decreasing the pressure in the
141 reservoir with a vacuum pump. After opening the valve to the sample, pressure first
142 increased, due to expansion of the gas from the sample tube to the reservoir, followed
143 by a slow increase due to desorption of HCl from the sample surface. After pressure
144 stabilized, the valve between reservoir and sample was closed and the procedure was
145 repeated, until the pressure in the reservoir was close to zero mbar. Measuring an
146 entire adsorption and desorption cycle for a sample took several weeks. Experiments
147 at 150 °C were carried out by immersing the sample tube in an oil bath; for
148 experiments at – 76 °C, the sample tube was cooled with a mixture of dry ice and
149 acetone. Main sources of error in the surface concentrations are the specific surfaces
150 of the powders, the pressures, and the volumes in the system.

Wet chemical analyses were carried out in order to confirm the measured HCl surface concentrations. About 10 g of HCl-loaded glass sample were mixed with 100 ml of distilled water and stirred for 24 hours in a closed Erlenmeyer flask. The solution was then filtered off and some NaHCO₃ added to adjust to neutral pH. Chloride was then determined by titrating against a 0.1 N AgNO₃ solution with Ag₂CrO₄ as endpoint indicator (Mohr method). Surface concentrations (in mg/m²) were then obtained by dividing the mass of measured HCl by the surface area of the sample according to the BET data.

3. Results

3.1. Kinetics of adsorption

Figure 1 shows the experimentally observed decrease of pressure during an adsorption experiment. For every adsorption step, the data can be described by an equation

$$(p - p_{eq}) = (p_0 - p_{eq}) e^{-\lambda t} \quad (1)$$

where p is pressure, p_{eq} is the equilibrium pressure, and p_0 is the initial pressure after opening the valve between gas reservoir and sample; λ is the rate constant and t is time. Values of p_{eq} and of λ were obtained by fitting equation (1) to the data for every adsorption step. Since in the ideal gas law, pressure is proportional to the number of moles in the gas phase, $(p - p_{eq})$ is proportional to the number of gas atoms n that still will be absorbed and $(p_0 - p_{eq})$ is proportional to the initial number of gas atoms n_0

that ultimately will end up on the sample surface. The above equation (1) is therefore equivalent to a first-order-law of reaction kinetics

$$n = n_0 e^{-\lambda t} \quad (2)$$

with the same rate constant λ as in equation (1).

Experimentally determined rate constants are compiled in Table 2; measured values for λ range from $2.13 \cdot 10^{-6} \text{ s}^{-1}$ to $1.80 \cdot 10^{-4} \text{ s}^{-1}$. The timescale for reaching equilibrium is in the order of magnitude of the inverse of these rate constants. For dacite at room temperature, a clear decrease of λ with the initial gas pressure of the adsorption experiment is observed. This may be related to the fact that in the experiments at higher pressure, the most reactive surface sites had already been saturated with HCl in the previous steps of the adsorption experiment. In other words, with increasing surface coverage of the sample, the rate of adsorption decreases. This effect is not so clearly seen for the other samples. Interestingly, the rate constants for HCl adsorption on dacite at $-76 \text{ }^\circ\text{C}$ are in most cases higher than at room temperature. This is unexpected, as reaction rates should generally increase with temperature. However, as will be discussed below, only the most reactive surface sites seem to be accessible for HCl adsorption at $-76 \text{ }^\circ\text{C}$, and this higher reactivity probably also translates into higher rate constants. Desorption experiments also followed a first-order-kinetics, with rate constants similar to those for adsorption on the same sample. However, only very little desorption was generally observed and therefore, desorption kinetics will not be further discussed.

3.2. Adsorption isotherms

Adsorption and desorption isotherms of HCl for andesitic, dacitic and rhyolitic glasses are shown in Figure 2. With increasing pressure, the amount of HCl adsorbed on the surface first increases sharply and then levels off and reaches a plateau. This behavior corresponds to a type I adsorption isotherm in the Brunauer classification (Brunauer et al. 1940), which is typical for a chemisorption process, where the adsorbed molecule forms strong chemical bonds with the substrate. Above about 500 mbar, there is a slight further increase in surface concentration that may indicate minor multilayer adsorption.

The desorption isotherms show that the adsorption process is nearly irreversible, i. e. the surface concentration of HCl remains nearly constant when pressure is decreased to zero mbar. This behavior is again consistent with a chemisorption process involving the formation of strong chemical bonds between HCl and the substrate. The HCl surface concentration observed for andesitic and rhyolitic glasses are rather similar, while those for the dacite glass are 2 to 3 times higher. Inspection of Table 1 shows that this effect cannot be due to the SiO_2 , Al_2O_3 , CaO or MgO contents of the glass, since the percentage of these components in the dacite glass is between that for rhyolite and andesite. However, the total alkali ($\text{Na}_2\text{O} + \text{K}_2\text{O}$) content of the dacite is significantly higher than for the other two compositions. Since the alkalis are the strongest bases in the system, it is plausible that they enhance the reaction with the acidic HCl molecule. This is consistent with the enhanced reactivity of alkali-rich glasses with HCl vapor at high-temperature, near vent conditions (Ayris et al. 2014). Note, however, that the alkali contents of the synthetic glasses used for this study are

not necessarily representative of a global average of rhyolite or dacite compositions and individual rhyolites may very well have higher total alkalis than some dacites.

The temperature dependence of HCl adsorption was explored for dacite, by carrying out additional experiments at -76 °C and at 150 °C. The results are shown in Figure 3. Adsorption increases with temperature, probably because at low temperature adsorption occurs only on some particularly reactive sites, with the number of available sites increasing with temperature. This is a typical behavior sometimes observed for chemisorption, where the formation of chemical bonds requires some activation energy that can only be overcome above a certain temperature (e.g. Batzill 2006, Duran-Munoz et al. 2013).

The surface concentrations of HCl remaining on the samples after the end of the desorption experiments, as derived from the measurements of the isotherms, were checked by argentometric titration of leachate solutions, with generally good agreement (Supplementary Table S1). Only the dacite sample from the experiment at room temperature may have lost some HCl by handling on humid air before the argentometric analysis. For the comparison, the surface concentrations were converted into wt. % using the specific surfaces given in Table 1.

3.3. A regression model for the adsorption of HCl on dacite glass

Schmauss and Keppler (2014) showed that the temperature and pressure dependence of the adsorption of SO₂ on volcanic ash may be described by a modified Freundlich isotherm

$$\ln c = A T^{-1} + B \ln p + C \quad (3)$$

where c is the surface concentration in mg/m^2 , T is temperature in K and p is the partial pressure of the absorbed gas in mbar. A least squares fit of all the experimental data for HCl adsorption on dacite glass using the same equation yielded $A = -715.3 \pm 55.3$, $B = 0.27 \pm 0.03$, and $C = 1.26 \pm 0.29$, with $R^2 = 0.93$. A comparison of measured and predicted surface concentrations of HCl is shown in Figure 4.

3.4. HCl adsorption on a natural obsidian sample

In order to test whether the adsorption data obtained by using synthetic samples are also applicable to natural, Fe-bearing volcanic glasses, we also measured the adsorption of HCl on a natural alkali-rhyolitic obsidian from the 1739 AD eruption of Vulcano (Aeolian Islands, Italy; see Table 1). This obsidian contains a small fraction of feldspar microlites. In adsorption experiments at room temperature, both the kinetics of adsorption and the adsorption isotherm were found to be quite similar to the synthetic glasses (Fig. 5). The HCl surface concentrations observed for the Vulcano obsidian are somewhat higher than for the synthetic rhyolite and resemble more those for synthetic dacite (Fig. 2). This is, however, entirely consistent with the elevated bulk alkali content in this sample, supporting the idea that this is the primary compositional parameter influencing HCl adsorption.

4. Discussion

4.1. Applicability of the experimental data to adsorption in volcanic plumes

The experiments in the present study were carried out in the presence of HCl alone, while in the volcanic plume, H₂O is usually the most abundant component, together with smaller amounts of SO₂, HCl and traces of other gases. CO₂ may be an abundant species as well, but since the CO₂ molecule lacks a permanent dipole moment, its absorption on surfaces can likely be ignored. The much more important question is therefore, whether the data obtained in the present study may be applied to the situation in a volcanic plume, where HCl is a minor component compared to H₂O. Very likely this is possible, because the glass powders used in the experiments described here were exposed to air of average humidity at ambient conditions during the preparation of the experiments. Both studies on synthetic silicate glasses and of volcanic ashes show that under ambient conditions and also in a volcanic plume, the surface of a glass particle will be covered with a complete layer of adsorbed H₂O molecules (Razouk and Salem 1948, Delmelle et al. 2005). Accordingly, there should be no difference in HCl surface concentration between the glass powders studied here in pure HCl alone and the adsorption of HCl on ash in the volcanic plume. Dissolution of HCl gas in liquid water adhering to ash particles is a separate effect, which will be discussed below.

Figure 6 compares Cl concentrations adsorbed on the surface of volcanic ashes from more than 40 individual eruptions with the experimental data for dacite glass obtained in this study. To convert surface concentrations (in mg/m²) into bulk concentrations (mg Cl / kg ash), the specific surface area of the ash has to be assumed. Figure 6 shows predicted maximum bulk concentrations (vertical lines) for two different specific surfaces of 1 m²/g, which is at the low end of this parameter for fine ash (Demelle et al. 2005; Gislason et al. 2011) and 0.1 m²/g, more characteristic for

coarser ash (see supplementary Table S2 for examples). The vertical lines in Figure 6 give maximum concentrations achievable at a given specific surface and temperature at high HCl partial pressures. However, inspection of Figure 3 shows that similar concentrations may already be reached at low HCl partial pressures (10 - 100 mbar) realistic for a volcanic plume. Figure 6 shows that adsorption of HCl from the gas phase can account for the vast majority of the observed Cl concentrations. Only the data for Irazu and San Miguel appear anomalously high, but they could still be explained by surface adsorption if the specific surface of these ashes were higher, in the order of 2 – 4 m²/g, within the range confirmed by measurements on fine ashes (Demelle et al. 2005; Gislason et al. 2011). More likely, however, these ashes contain Cl from some other source, e.g. from hydrothermal alteration. Alteration processes may also have contributed some Cl to other samples. The data shown in Figure 6 are completely consistent with earlier experimental results for fluorine. Oskarsson (1980) already concluded that the fluorine concentrations adsorbed on ash may be explained by adsorption from the gas phase at relatively low temperatures near 200 °C.

In a volcanic plume, ash may interact with aerosols or become coated by films of liquid water or ice. Rose (1977) suggested that the accumulation of aerosol particles, particularly of H₂SO₄ is a main source for adsorbed material on ash. However, H₂SO₄ aerosols are usually only a minor species, subordinate to SO₂ in volcanic plumes close to the vent (e.g. Mather et al. 2006). Delmelle et al. (2007; see also Gislason et al. 2011) detected Cl and S on the surface of ash particles by X-ray photoelectron spectroscopy, but not by SEM. They concluded that Cl and S form coatings with a thickness of a few nm at most; they further suggested that this observation together

with the observed surface depletion in Na, K, Mg, and Ca argues against the deposition of material via aerosols, but is more consistent with precipitation from a liquid film. However, their data are equally consistent with our model of direct adsorption from a gas phase, since the shape of the adsorption isotherms indeed suggests the formation of a mono-molecular layer of HCl on the ash surface. Coating of ash particles by water certainly occurs in some parts of the plume, but this process is reversible. Once the water evaporates, the dissolved HCl and SO₂ will also be lost, unless some surface reaction has occurred. However, if the surface is in equilibrium with the liquid film and the liquid is in equilibrium with a gas phase, then the surface is also in direct equilibrium with the gas. In other words, this process should lead to the same surface concentration as observed in our experiments. The fact that surface reactions, but not the solubility in liquid water determine the origin of leachable material on ash surfaces is also supported by the observation of a systematic offset between S/Cl ratios adsorbed on ash and S/Cl ratios in rainwater (Edmonds et al., 2003). If the relative solubility of SO₂ and HCl in liquid water somehow determined the S/Cl ratio on the ash surface, this ratio should be the same as in rainwater that had interacted with the plume.

4.2 Deriving volcanic gas compositions from adsorbate analyses

The analysis of volatile species adsorbed on fresh ash surfaces is a convenient and frequently used method to infer volcanic gas compositions (e.g. Rose 1977, Williams et al. 1986, Armienta et al. 1998, de Hoog et al. 2001, Armienta et al. 2010, Bagnato et al. 2011, 2013). Usually, the implicit assumption is made that the concentration ratio of adsorbed S, Cl, and F is somehow comparable to the molar ratio of the

corresponding species in the gas phase of the plume. Our experimental data, together with published results for the adsorption of SO₂ on volcanic ash (Schmauss and Keppler, 2014) allow testing this assumption. The adsorption of HCl and SO₂ can likely be treated independently, without considering direct interactions, because the concentration of these gases, particularly in the dilute part of the plume, is very low and therefore, none of them will fully cover the glass surface. Moreover, the experimental data of this study and of Schmauss and Keppler (2014) suggest that HCl and SO₂ actually react with different surface sites, since both the dependence of adsorption on glass composition and on temperature are very different. For SO₂, glass composition has little influence on adsorption, while the total alkali content seems to control the reactivity with HCl. HCl adsorption increases with temperature, while the adsorption of SO₂ decreases with temperature.

Schmauss and Keppler (2014) showed that SO₂ adsorption on dacite glass can be described by the equation

$$\ln c_{\text{SO}_2} = 2140 T^{-1} + 0.29 \ln p_{\text{SO}_2} - 9.32 \quad (4)$$

while in the present study, we observed that HCl adsorption follows the equation

$$\ln c_{\text{HCl}} = -715.3 T^{-1} + 0.27 \ln p_{\text{HCl}} + 1.26 \quad (5)$$

In both equations, the coefficient in front of the $\ln p$ term is indistinguishable within experimental error. If one assumes an average coefficient of 0.28, both equations can be combined to

$$\ln (c_{\text{SO}_2}/c_{\text{HCl}})_{\text{adsorbed}} = 2855 T^{-1} + 0.28 \ln (p_{\text{SO}_2}/p_{\text{HCl}}) - 10.58 \quad (6)$$

At the low pressures involved, the ratio of the partial pressures $p_{\text{SO}_2}/p_{\text{HCl}}$ is virtually identical with the SO_2/HCl molar ratio in the gas. To convert the ratio of surface concentrations $c_{\text{SO}_2}/c_{\text{HCl}}$, which are given in mg/m^2 , into a molar ratio of S/Cl, the numbers have to be divided by the ratio of the molar masses of SO_2 and HCl . This adds a linear term of $-\ln (64.06/36.46) = -0.56$ to the equation, which then becomes:

$$\ln (S/Cl)_{\text{adsorbed}} = 2855 T^{-1} + 0.28 \ln (S/Cl)_{\text{gas}} - 11.14 \quad (7)$$

where S/Cl now refers to the molar ratio in the gas and on the glass surface.

Figure 7 shows the ratio of S/Cl on dacitic ash surfaces, as predicted by equation 7 for a range of temperatures and gas compositions. Obviously, the adsorbed S/Cl ratio is a very strong function of temperature. In fact, the temperature effect is much stronger than the effect of the S/Cl ratio in the gas. For example, near 0 °C, increasing the S/Cl ratio in the gas by a factor of 10 has the same effect on the absorption as reducing temperature by less than 20 °C. The relatively small effect of gas composition is due to the factor of 0.28 in front of the $\ln (S/Cl)_{\text{gas}}$ term in equation (7); it implies that under otherwise equal conditions, (S/Cl) in the adsorbate only increases by a factor of $(S/Cl)_{\text{gas}}^{0.28}$, i.e. a 10-fold increase in this ratio in the gas phase only translates into a less than 2-fold increase in the adsorbate. The 0.28 exponent is related to the effect seen in Figure 2 that the amount of adsorbed HCl first increases sharply at low p_{HCl} , but then levels off at higher p_{HCl} . The strong effect of temperature on the adsorbed

S/Cl ratio is obviously related to the opposite temperature dependence for HCl and SO₂ adsorption. The decrease of adsorption with temperature for SO₂ (Schmauss and Keppler 2014) is the normal behavior expected for adsorption. This is because in the expression for the Gibbs free energy $\Delta G = \Delta H - T\Delta S$ for the adsorption reaction, the $-T\Delta S$ term increases with temperature and should therefore shift the equilibrium to the side with higher entropy; the entropy of a molecular species is always higher in the gas phase than adsorbed on a surface. The increase in HCl adsorption with temperature is therefore very unusual, but this kind of behavior is sometimes observed for chemisorption (e.g. Batzill 2006, Duran-Munoz et al. 2013), i.e. if the adsorption process involves the formation of strong chemical bonds. In such a situation, an activation energy may have to be overcome for the reaction, so that only a fraction of sites is involved in the adsorption process at low temperature, while this fraction increases at higher temperatures. Once all possible surface sites are activated, adsorption should decrease upon further increase with temperature, because of the thermodynamic argument mentioned above. Accordingly, the data presented here for HCl adsorption and equation 7 should not be extrapolated to temperatures far above those for which they were calibrated (i.e. beyond 150 °C).

The strong temperature effect on adsorption as shown in Figure 7 needs to be taken into account whenever volcanic gas compositions are to be derived from analyses of volatile species adsorbed on ash surfaces. This means that estimates of volcanic fluxes of HCl that were obtained from SO₂ flux measurements scaled by the S/Cl ratio in adsorbates should be treated with considerable caution; the same may also apply to other gas species. The frequently made assumption of equal adsorption of different species is only valid under very specific conditions (see also Bagnato et al. 2011). For

example, Figure 7 shows that for a gas with an S/Cl ratio of 1, equal adsorption, resulting in an S/Cl ratio of 1 also in the adsorbate, only occurs at a temperature near -20°C . However, for an S/Cl ratio in the gas of 10, the temperature where no fractionation occurs decreases to near -50°C .

The conclusions reached here on the strong effect of temperature on the fractionation of SO_2 and HCl during adsorption are actually quite consistent with a number of field observations. S/Cl ratios of ashes vary widely, < 0.01 to > 100 , and often by orders of magnitude even within the same eruption (see Supplementary Table 2). This is likely not only due to variations in gas composition, but also to the fractionation of S and Cl between gas and ash. Edmonds et al. (2003) measured the SO_2/HCl ratio of gases from three eruption periods of the Soufrière Hills volcano on Montserrat between 1996 and 2002, using both open path infrared spectroscopy and the analysis of ash leachates. For the phase I and phase II major dome building periods, a SO_2/HCl molar ratio near 0.1 was spectroscopically detected in the plume and ash analyses gave similar (although more scattered) numbers. This is consistent with Figure 7, which suggests that for an S/Cl ratio of 0.1, no fractionation occurs between ash and gas phase near $+30^{\circ}\text{C}$ – a very plausible temperature for a low-altitude tropospheric plume in a tropical climate. Bagnato et al. (2013) studied ash leachates of the 2010 Eyafjallajökull eruption on Iceland and found major discrepancies between the S/Cl ratio adsorbed on ash surfaces and that measured in the volcanic gases. For the highly explosive phase III eruption, S/Cl ratios from ash leachates are mostly between 0.4 and 0.6, while direct gas measurements yielded significantly higher molar S/Cl ratios of 1.5 – 3.3. Inspection of Figure 7 suggests that these data may be reconciled by assuming a temperature of adsorption near 0°C , quite plausible for a tropospheric

plume during spring in Iceland. Note that these ash samples were taken at horizontal distances from the vent up to more than 50 km, where the plume will have cooled down to ambient atmospheric temperature; closer to the vent, larger variations in adsorbed S/Cl ratio are observed, which may be related to variations in plume temperature and also plume height (4 – 9 km; Petersen et al. 2012). Even larger fractionations of S and Cl between ash and gas were observed for the basaltic fire fountain phase; the S/Cl ratio in the gas was measured to be between 5 and 25 while a molar ratio of S/Cl of 0.14 was measured on the ash. According to Figure 7, this could imply equilibration between gas and ash at temperatures around + 50 °C, which is plausible for a fire fountain eruption, as there may be very significant radiative heating of particles after they left the vent and the plume likely entrained less ambient air than for the highly explosive phase III.

In the previous discussion, we have referred to Figure 7, which is based on equation 7 and strictly valid only for a dacitic composition. Glass composition will have some effect on the S/Cl fractionation, which needs to be considered. However, this effect is much smaller than the variation due to temperature. For a given gas composition, Figure 7 suggests variations in the ratio of adsorbed S and Cl by four orders of magnitude over just 250 °C. Compared to this, the compositional effect on the amount of adsorbed HCl (Fig. 2) is only about a factor of 2 and the effect of glass composition on SO₂ adsorption is even smaller (Schmauss and Kepper 2014). Therefore, we believe that the conclusions derived from comparing the curves in Figure 7 with ash leachate analyses are at least approximately correct, although additional calibrations of the effect of ash composition on the S/Cl fractionation between plume gas and ash surface are certainly desirable. In general, our discussion

shows that a large part of the apparent discrepancies between gas composition and the composition of gas leachates can be accounted for by the effect of temperature on adsorption. This does not rule out that other factors, in particular alteration processes may also be important under some circumstances. However, for fresh, unaltered ash it may indeed be possible to derive gas compositions from leachate analyses, if reasonable estimates of plume temperature can be made. Moreover, on a local scale close to a vent, the S/Cl ratio may actually provide a sensitive thermometer for the temperature in the plume.

4.3. Stratospheric HCl yield and ozone depletion

With the experimental data on HCl adsorption obtained in this study, the fraction of volcanic HCl reaching the stratosphere during Plinian eruptions can be better constrained. As noted above, HCl adsorption increases with temperature, at least up to 150 °C. Accordingly, one may suspect that most of the adsorption may occur in the relatively hot parts of the volcanic plume. However, ascent velocities in a typical Plinian eruption column are $> 100 \text{ m s}^{-1}$ (Textor et al. 2006), implying that ash particles reach the stratosphere within 1 – 2 minutes. This very much limits the time available for high-temperature, near-vent interaction between volcanic gases and ash. The highest rate constant for HCl adsorption measured in this study (Table 4) was $1.8 \cdot 10^{-4} \text{ s}^{-1}$. For a residence time of 120 s, this would allow only 2 % of the equilibrium surface concentration to be adsorbed on the ash. Accordingly, it is likely that most of the adsorption occurs in the dilute parts of the volcanic plumes after it has cooled down to the ambient temperature at the respective altitude.

498 A rough estimate of the magnitude of HCl adsorption can be obtained by considering
499 the HCl surface concentration that would result from the (hypothetical) total
500 adsorption of all the HCl in the plume. This concentration is simply the ratio of the
501 total mass of HCl in the plume to the total available surface area of the ash. According
502 to Woods and Bursik (1991) fine ash with a grain size $< 100 \mu\text{m}$ accounts for > 50 wt.
503 % of total deposit for Plinian eruptions. Measurements of fine ash samples from
504 various volcanoes yielded specific surfaces of $1.1 - 2.1 \text{ m}^2 / \text{g}$ (Delmelle et al. 2005).
505 The ash is produced by the exsolution of gas bubbles, which ultimately disrupt and
506 fragment the melt. Subduction zone magmas that are responsible for the most
507 prominent explosive eruptions typically have pre-eruptive water contents near 5 wt. %
508 (e.g. Métrich and Wallace 2008). Water is also the main component of the gas plume,
509 with HCl concentrations ranging from < 0.05 to > 5 mole %, the majority of data
510 probably being in the 0.1 to 1 mole % range (Symonds et al. 1994, Fischer 2008).
511 These data from volcanic gases are in rough agreement with the Cl/ H_2O ratio in melt
512 inclusions from primitive arc basalts (Métrich and Wallace 2008). If one therefore
513 assumed a mass ratio of volcanic gas to (glassy) ash of 0.05 (equivalent to 5 % H_2O in
514 the pre-eruptive magma), 1 mole % HCl in the gas and a surface of $1 \text{ m}^2/\text{g}$ for the
515 total ash (or 50 % of fine ash with $2 \text{ m}^2/\text{g}$), adsorbing all the HCl on the ash would
516 yield a surface concentration of $1.01 \text{ mg}/\text{m}^2$. Comparing this number to the
517 experimental data in Figure 2 and 3 suggests that such surface concentrations may be
518 easily reached at room temperature or above; however, they may not be achievable at
519 the much lower temperatures prevailing in the stratosphere. The situation would be
520 very different, however, for an initial HCl concentration in the gas of 0.1 mole %; the
521 corresponding surface concentration of $0.10 \text{ mg}/\text{m}^2$ is easily reached even at low
522 temperatures and at low HCl partial pressure. This rough calculation already shows

that the initial HCl concentration in the plume, which likely reflects the pre-eruptive Cl/H₂O ratio in the magma, largely controls the fraction of HCl sequestered by ash and therefore, together with scavenging by hydrometeors, the effective stratospheric HCl loading.

For a fully quantitative treatment of HCl adsorption, the equilibrium between the gas phase and ash surface as described by equation (5) has to be considered together with mass balance constraints under the conditions prevailing in the umbrella part of a volcanic plume. For our calculations, we assume a plume model similar to that described by Textor et al. (2006). The umbrella part of the plume is located at an altitude near 20 km with a temperature around 220 K, containing about 100 g of ash per kg of plume mixture. Assuming an initial gas mass fraction in the erupting material of 5 wt. % (see above), this implies a dilution of volcanic gases by entrained air by a factor of 200. The calculations are, however, rather insensitive to this dilution factor, since according to equation (5), adsorption only increases with $p_{\text{HCl}}^{0.27}$, i.e. a ten-fold increase in the dilution factor would only decrease adsorption by a factor of 1.9. For a volcanic gas with 1 mole % HCl, the partial pressure of HCl decreases from 10 mbar at the vent to 0.0022 mbar in the umbrella cloud by the combined effects of the increasing altitude and dilution by entrained air. This number does not include possible scavenging of HCl by hydrometeors (see Textor et al. 2003). Under the given conditions, equation (5) predicts a concentration of HCl adsorbed on the surface of ash of 0.026 mg/m² in equilibrium with this HCl partial pressure, less than 3 % of the 1.01 mg/m² required for total adsorption (see above). Since during the adsorption process, the partial pressure of HCl in the gas decreases until equilibrium is reached, the real number for the equilibrium surface concentration is slightly smaller.

Following the method described by Schmauss and Keppler (2014), one obtains virtually the same value of 0.026 mg/m^2 . This number appears small, but the resulting bulk Cl concentration (26-52 mg/kg for a specific surface of $1\text{-}2 \text{ m}^2/\text{g}$) overlaps well with the low end of concentrations reported for natural ashes (Fig. 6). Stratospheric ash samples are likely under-represented in Figure 6, because many eruptions did not reach the stratosphere and even for large eruptions, the ashes likely contain particles that did not reach the stratosphere. For less explosive eruptions, particle velocities are smaller and the plume may be less diluted by entrained air. Ash might therefore be exposed to higher HCl partial pressures for longer times and at higher temperatures, leading to stronger adsorption. This is a possible explanation for the fact that the surface concentrations predicted for adsorption in the stratosphere are at the lower end of the data for natural ash samples. However, the physical conditions for adsorption likely vary considerably between individual eruptions and are influenced by parameters such as the actual wind field that are hard to include in general models.

The calculation above clearly shows that for high initial HCl concentrations (> 1 mole %) in the gas phase of a Plinian eruption, adsorption by ash does not significantly reduce the stratospheric HCl loading. However, the adsorption effect becomes significant for low initial HCl concentrations. For example, for an initial HCl content in the volcanic gas of 0.1 mole %, an equilibrium surface concentration of 0.013 mg/m^2 is obtained, 13 % of the value required for total absorption (see above). The relationship between HCl content in the initial volcanic gas and the adsorption on ash is illustrated in Figure 8. Physically, this relationship is due to the fact that the total amount of HCl in the plume increases proportionally to the initial HCl molar fraction and therefore the HCl partial pressure; however, the amount of

HCl adsorbed on ash only increases with $p_{\text{HCl}}^{0.27}$ so that at higher p_{HCl} , the fraction of HCl that is not removed by adsorption increases. In general, the efficiency of adsorption on ash surfaces in dilute eruption plumes is much smaller for HCl than for SO_2 (Schmauss and Keppler 2014).

The pre-eruptive Cl contents and Cl/ H_2O ratios in subduction zone volcanics tend to be high (Métrich and Wallace 2008, Kutterolf et al. 2013). Accordingly, HCl contents in the fluid phase near 1 mole % and higher will be common for Plinian eruptions in subduction zone settings. In such a situation, HCl adsorption on ash will not be able to significantly reduce the amount of HCl reaching the stratosphere. Although there is still much work to be done to understand these processes, previous studies (Textor et al. 2003) have suggested limited efficiency of HCl scavenging by liquid water and by ice in the eruption column, with more than 25 % of the total HCl reaching the stratosphere. Our results therefore support the hypothesis that significant and perhaps even catastrophic ozone depletion due to the HCl yield of giant eruptions is possible (Kutterolf et al. 2013, Black et al. 2014).

5. Conclusions

The interaction of volcanic gases with ash particles could potentially limit the environmental impact of explosive eruptions. We provide new experimental data on the kinetics and thermodynamics of HCl adsorption on volcanic ash. Unlike for SO_2 , HCl adsorption increases with temperature, so that large temperature-dependent fractionations between HCl and SO_2 occur during the adsorption process. Extracting volcanic gas compositions from analyses of ash leachates therefore requires correcting for this effect. Although HCl adsorption increases with temperature, the

slow rate of the process implies that most of the adsorption occurs in the cold, dilute parts of a volcanic plume. For low initial HCl concentrations in the volcanic gas (0.1 mole % and below), the depletion of HCl by adsorption can be significant. However, for HCl concentrations of 1 mole % and above, adsorption on ashes is unlikely to reduce the stratospheric HCl yield of Plinian eruptions. Therefore, it appears quite plausible that the HCl yield of large explosive eruptions may cause significant ozone depletion in the stratosphere.

Acknowledgements

We would like to thank Gerti Gollner and Julia Huber for technical assistance in the adsorption experiments and Lena Geiling for the determination of specific surfaces. Constructive reviews by Tamsin Mather, Steffen Kutterolf and an anonymous referee helped to improve the manuscript.

References

- Armienta, M.A., Martin-Del-Pozzo, A. L., Espinasa, R., Cruz, O., Cenicerros, N., Aguayo, A., Butron, M.A., 1998. Geochemistry of ash leachates during the 1994-1996 activity of Popocatépetl volcano. *Appl. Geochem.* 13, 841-850.
- Armienta, M.A., de la Cruz-Reyna, S., Soler, A., Cruz, O., Cenicerros, N., Aguayo, A., 2010. Chemistry of ash-leachates to monitor volcanic activity: An application to Popocatépetl volcano, central Mexico. *Appl. Geochem.* 25, 1198–1205.
- Ayris, P.M., Delmelle, P., Cimarelli, C., Maters, E.C., Suzuki, Y.J., Dingwell, D.B., 2014. HCl uptake by volcanic ash in the high temperature eruption plume: Mechanistic insights. *Geochim. Cosmochim. Acta* 144, 188-201.

- 622 Bagnato, E., Aiuppa, A., Andronico, D., Cristaldi, A., Liotta, M., Brusca, L.,
 623 Miraglia, L., 2011. Leachate analyses of volcanic ashes from Stromboli volcano:
 624 A proxy for the volcanic gas plume composition? J. Geophys. Res. 116, D17204,
 625 DOI: 10.1029/2010JD015512.
- 626 Bagnato, E., Aiuppa, A., Bertagnini, A., Bonadonna, C., Cioni, R., Pistolesi, M.,
 627 Pedone, M., Hoskuldson, A., 2013. Scavenging of sulphur, halogens and trace
 628 metals by volcanic ash: The 2010 Eyjafjallajökull eruption. Geochim.
 629 Cosmochim. Acta 103, 138-160.
- 630 Batzill, M., (2006) Surface science studies of gas sensing materials: SnO₂. Sensors 6,
 631 1345-1366.
- 632 Black, B.A., Lamarque, J.F., Shields, C.A., Elkins-Tanton, L.T., Kiehl, J.T., 2014.
 633 Acid rain and ozone depletion from pulsed Siberian Traps magmatism. Geology
 634 42, 67-70.
- 635 Brasseur, G., Granier, C., 1992. Mount Pinatubo aerosols, chlorofluorocarbons, and
 636 ozone depletion. Science 257, 1239-1242.
- 637 Brunauer, S., Deming, L.S., Deming, W.E., Teller, E., 1940. On a theory of the van
 638 der Waals adsorption of gases. J. Am. Chem. Soc. 62, 1723-1732.
- 639 de Hoog, J.C.M., Koetsier, G.W., Bronto, S., Sriwana, T., van Bergen, M.J. 2001.
 640 Sulfur and chlorine degassing from primitive arc magmas: temporal changes
 641 during the 1982-1983 eruptions of Galunggung (West Java, Indonesia). J.
 642 Volcanol. Geothermal Res. 108, 55-83.
- 643 Delmelle, P., Villi  ras, F., Pelletier, M., 2005. Surface area, porosity and water
 644 adsorption properties of fine volcanic ash particles. Bull. Volcanol. 67, 160-169.

- 645 Delmelle, P., Lambert, M., Dufrêne, Y., Gerin, P., Óskarsson, N., 2007. Gas/aerosol–
 646 ash interaction in volcanic plumes: New insights from surface analyses of fine
 647 ash particles *Earth Planet. Sci. Lett.* 259, 159–170.
- 648 Duran-Munoz, F., Romero-Ibarra, I., Pfeiffer, H. (2013) Analysis of the CO₂
 649 chemisorption reaction mechanism in lithium oxosilicate (Li₈SiO₆): a new option
 650 for high-temperature CO₂ capture. *J. Materials Chem. A* 1, 3919-3925.
- 651 Edmonds, E., Oppenheimer, C., Pyle, D.M., Herd, R.A., 2003. Rainwater and ash
 652 leachate analysis as proxies for plume chemistry at Soufrière Hills volcano,
 653 Montserrat. In: Oppenheimer, C., Pyle, D.M., Barclay, J. (eds) *Volcanic*
 654 *Degassing*. Geological Society, London, Special Publications 213, 203-218.
- 655 Fischer, T. P., 2008. Fluxes of volatiles (H₂O, CO₂, N₂, Cl, F) from arc volcanoes.
 656 *Geochem. J.* 42, 21-38.
- 657 Gislason, S. R., Hassenkam, T., Nedel, S., Bovet, N., Eiríksdóttir, E. S., Alfredsson,
 658 H. A., Hem, C. P., Balogh, Z. I., Dideriksen, K., Óskarsson, N., Sigfusson, B.,
 659 Larsen, G., Stipp, S. L. S., 2011. Characterization of Eyjafjallajökull volcanic
 660 ash particles and a protocol for rapid risk assessment. *Proc Nat. Acad. Sci. USA*
 661 108, 7307-7312.
- 662 Halmer, M.M., Schmincke, H.U., Graf, H.F., 2002. The annual volcanic gas input into
 663 the atmosphere, in particular into the stratosphere: a global data set for the past
 664 100 years. *J. Volcanol. Geothermal Res.* 115: 511-528
- 665 Hofmann, D.J., Oltmans, S.J., Komhyr, W.D., Harris, J.M., Lathrop, J.A., Langford,
 666 A.O., Deshler, T., Johnson, B.J., Torres, A., Matthews, W.A., 1994. Ozone loss
 667 in the lower stratosphere over the United States in 1992 – 1993: Evidence for
 668 heterogeneous chemistry on the Pinatubo aerosol. *Geophys. Res. Lett.* 21, 65-68.

- 669 Kutterolf, S., Hansteen, T.H., Appel, K., Freundt, A., Krüger, K., Pérez, W.,
 670 Wehrmann, H. 2013. Combined bromine and chlorine release from large
 671 explosive volcanic eruptions: A threat to stratospheric ozone? *Geology* 41, 707-
 672 710.
- 673 Mankin, W.G., Coffey, M.T., 1984. Increased stratospheric hydrogen chloride in the
 674 El Chicon cloud. *Science* 226, 170-172.
- 675 Mankin, W.G., Coffey, M.T., Goldman, A., 1992. Airborne observations of SO₂, HCl,
 676 and O₃ in the stratospheric plume of the Pinatubo volcano in July 1991. *Geophys.*
 677 *Res. Lett.* 19, 179-182.
- 678 Mather, T.A., McCabe, J.R., Rai, V.K., Thiemens, M.H., Pyle, D.M., Heaton, T.H.E.,
 679 Sloane, H.J., Fern, G.R., 2006. Oxygen and sulfur isotopic composition of
 680 volcanic sulfate aerosol at the point of emission. *J. Geophys. Res.* 111, Article
 681 Number: D18205, DOI: 10.1029/2005JD006584
- 682 McCormick, M.P., Thomason, L.W., Trepte, C.R., 1995. Atmospheric effects of the
 683 Mt Pinatubo eruption. *Nature* 373: 399-404.
- 684 Métrich, N., Wallace, P.J., 2008. Volatile abundances in basaltic magmas and their
 685 degassing paths tracked by melt inclusions. *Rev. Mineral. Geochem.* 69, 363-402.
- 686 Millard, G. A., Mather, T. A., Pyle, D. M., Rose, W. I., Thornton, B., 2006. Halogen
 687 emissions from a small volcanic eruption: Modeling the peak concentrations,
 688 dispersion, and volcanically induced ozone loss in the stratosphere. *Geophys.*
 689 *Res. Lett.*, 33, Article number L19815, doi:10.1029/2006GL026959.
- 690 Oskarsson, N., 1980. The interaction between volcanic gases and tephra: fluorine
 691 adhering to tephra of the 1970 Hekla eruption. *J. Volcanol. Geoth. Res.* 8, 251–
 692 266.

- 693 Petersen, G.N., Bjornsson, H., Arason, P., 2012. The impact of the atmosphere on the
 694 Eyjafjallajökull 2010 eruption plume. *J. Geophys. Res. Atmospheres* 117, DOI:
 695 10.1029/2011JD016762.
- 696 Pyle, D.M., Mather, T.A., 2009. Halogens in igneous processes and their fluxes to the
 697 atmosphere and oceans from volcanic activity: A review. *Chem. Geology* 263,
 698 110-121.
- 699 Razouk, R.I., Salem, A.S., 1948. The adsorption of water vapor on glass surfaces. *J.*
 700 *Phys. Chem.* 52, 1208–1227.
- 701 Robock, A., 2000. Volcanic eruptions and climate. *Rev. Geophys.* 38, 191-219.
- 702 Rose, W.I., 1977. Scavenging of volcanic aerosols by ash: Atmospheric and
 703 volcanologic implications. *Geology* 5, 621-624
- 704 Rose, W.I., Millard, G.A., Mather, T.A., Hunton, D.E. Anderson, B., Oppenheimer,
 705 C., Thornton, B.F., Gerlach, T.M., Viggiano, A.A., Kondo, Y., Miller, T.M.,
 706 Ballenthin, J.O., 2006. Atmospheric chemistry of a 33–34 hour old volcanic
 707 cloud from Hekla Volcano (Iceland): Insights from direct sampling and the
 708 application of chemical box modeling. *J. Geophys. Res.* 111, article number
 709 D20206, doi:10.1029/2005JD006872.
- 710 Schmauss, D., Keppler, H., 2014. Adsorption of sulfur dioxide on volcanic ashes.
 711 *Am. Mineral.* 99, 1085–1094.
- 712 Solomon, S., Sanders, R.W., Garcia, R.R., Keys, J.G., 1993. Increased chlorine
 713 dioxide over Antarctica caused by volcanic aerosols from Mount Pinatubo.
 714 *Nature* 363: 245-248.
- 715 Solomon, S., Portmann, R.W., Garcia, R.R., Randel, W., Wu, F., Nagatani, R.,
 716 Gleason, J., Thomason, L., Poole, L.R., McCormick, M.P., 1998. Ozone

- 717 depletion at mid-latitudes: Coupling of volcanic aerosols and temperature
 718 variability to anthropogenic chlorine. *Geophys. Res. Lett.* 25, 1871-1874.
- 719 Symonds, R.B., Rose, W.I., Reed, M.H., 1988. Contributions of Cl- and F-bearing
 720 gases to the atmosphere by volcanoes. *Nature* 334, 415-418.
- 721 Symonds, R.B., Rose, W.I., Bluth, G.J.S., Gerlach, T.M., 1994. Volcanic-gas studies:
 722 Methods, results, and applications. *Rev. Mineral.* 30, 1-66.
- 723 Tabazadeh, A., Turco, R.P., 1993. Stratospheric chlorine injection by volcanic
 724 eruptions: HCl scavenging and implications for ozone. *Science*, 260, 1082–1086.
- 725 Textor, C., Graf, H.F., Herzog, M., Oberhuber, J.M., 2003. Injection of gases into the
 726 stratosphere by explosive volcanic eruptions. *J. Geophys. Res.* 108, Article
 727 number 4606, doi:10.1029/2002JD002987.
- 728 Textor, C., Graf, H.F., Herzog, M., Oberhuber, J.M., Rose, W.I., Ernst, G.G.J., 2006.
 729 Volcanic particle aggregation in explosive eruption columns. Part II: Numerical
 730 experiments. *J. Volcanol. Geothermal Res.* 150, 378-394.
- 731 Thamban, M., Chaturvedi, A., Rajakumar, A., Naik, S.S., D'Souza, W., Sing, A.,
 732 Rajan, S., Ravindra, R., 2006. Aerosol perturbations related to volcanic eruptions
 733 during the past few centuries as recorded in an ice core from the Central
 734 Dronning Maud land, Antarctica. *Current Science* 91, 1200-1207.
- 735 Wagnon, P., Delmas, R. J., Legrand, M., 1999. Loss of volatile acid species from
 736 upper firn layers at Vostok, Antarctica. *J. Geophys. Res.* 104, 3423–3431.
- 737 Wallace, L., Livingston, W., 1992. The effect of the Pinatubo cloud on hydrogen-
 738 chloride and hydrogen-fluoride. *Geophys. Res. Lett.* 19, 1209-1209.
- 739 Williams, S.N., Stoiber, R.E., Garcia, N., Londono, A., Gemmel, B.C., Lowe, D. R.,
 740 Connor, C.B., 1986. Eruption of the Nevado des Ruiz volcano, Colombia on 13
 741 November 1985: Gas flux and fluid geochemistry. *Science* 233, 964-967.

- 742 Woods, A.W., Bursik, M. I., 1991. Particle fallout, thermal disequilibrium and
743 volcanic plumes. *Bull. Volcanol.* 53, 559-570.
- 744 Woods, D.C., Chuan, R.L., Rose, W.I. , 1985. Halite particles injected into the
745 stratosphere by the 1982 El Chicón eruption. *Science* 230, 170-172.
- 746 Zdanowicz, C. M., Zielinski, G. A., Germani, M. S., 1999. Mount Mazama eruption:
747 Calendrical age verified and atmospheric impact assessed. *Geology* 27, 621– 624.
748

749 **Table 1**

750 Chemical composition (wt. %) and specific surface A (m²/g) of synthetic glass
 751 samples and of a natural obsidian from Vulcano (Aeolian Islands, Italy) used for
 752 adsorption experiments

	Rhyolite	Dacite	Dacite	Dacite	Andesite	Vulcano
		Batch 1	Batch 2	Batch 3		Obsidian
SiO ₂	76.45 (83)	67.08 (30)	67.02 (49)	66.68 (71)	56.77 (18)	73.47 (35)
Al ₂ O ₃	12.37 (53)	16.49 (21)	16.81 (23)	16.96 (32)	21.63 (13)	13.49 (22)
Fe ₂ O ₃ (t)						1.86 (13)
MgO	3.14 (24)	4.96 (15)	4.97 (23)	5.14 (37)	7.31 (16)	0.11 (04)
CaO	0.80 (07)	2.80 (10)	2.93 (11)	2.86 (16)	7.46 (10)	0.83 (10)
Na ₂ O	2.77 (08)	4.31 (09)	4.20 (05)	4.46 (09)	3.88 (09)	4.42 (08)
K ₂ O	3.33 (05)	3.15 (06)	3.00 (06)	2.92 (07)	1.77 (06)	5.10 (05)
Total	98.86	98.79	98.93	99.02	98.82	99.28
A	3.82	4.90	1.50	2.74	3.01	2.97

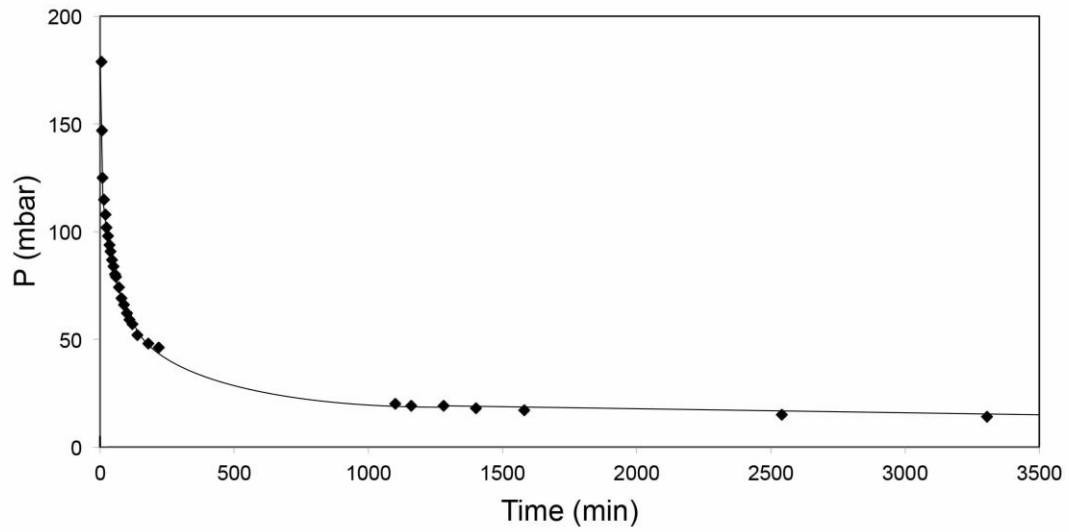
753 Numbers in parentheses are one standard deviation in the last digits. Fe₂O₃ (t) is the
 754 total iron content given as Fe₂O₃. For dacite, three batches of sample were prepared.
 755 Batch 1 was used for experiments at room temperature, batch 2 at 150 °C, and batch 3
 756 at -76 °C. Note that the synthetic compositions do not necessarily correspond to
 757 global averages of the respective rock type.

758 **Table 2**759 Rate constants λ for the adsorption of HCl on glass surfaces

Andesite		Dacite				Rhyolite			
T = 22 °C		T = - 76 °C		T = 22 °C		T = 150 °C		T = 22 °C	
p (mbar)	λ (10^{-6} s $^{-1}$)	p (mbar)	λ (10^{-6} s $^{-1}$)	p (mbar)	λ (10^{-6} s $^{-1}$)	p (mbar)	λ (10^{-6} s $^{-1}$)	p (mbar)	λ (10^{-6} s $^{-1}$)
68	124 (48)	58	58.5 (3.6)	42	180 (24)	104	44.4 (1.3)	80	45.4 (5.5)
105	52.1 (11.2)	86	103 (9)	147	32.1 (1.4)	95	15.9 (0.5)	125	57.0 (9.7)
185	44.3 (9.3)	123	96.7 (6.4)	197	12.0 (0.3)	315	14.8 (1.1)	191	149 (3)
374	28.2 (8.1)	206	99.4 (6.3)	306	5.98 (1.41)	424	6.92 (0.28)	243	37.7 (13.7)
581	42.8 (11.4)	299	103 (7)	528	6.32 (0.27)	538	25.4 (0.3)	371	43.0 (17.0)
721	117 (23)	529	92.6 (10.7)	692	7.58 (0.72)	798	21.8 (25.8)	506	46.3 (14.1)
852	58.6 (10.2)	723	66.2 (30.0)	794	2.75 (7.06)	956	18.1 (19.0)	713	34.0 (12.6)
982	36.4 (15.7)	935	76.1 (23.3)	965	2.13 (0.43)			967	37.3 (14.5)

760 p is the initial pressure of HCl vapor to which the sample was exposed in each step. The pressures are listed in the sequence of the steps of the

761 adsorption experiment. Numbers in brackets are estimated uncertainties.



762

763

764 **Fig. 1.** Kinetics of HCl adsorption on dacitic glass at room temperature and for an
765 initial pressure $p_0 = 179$ mbar. Pressure in the system decreases exponentially, until
766 equilibrium is reached.

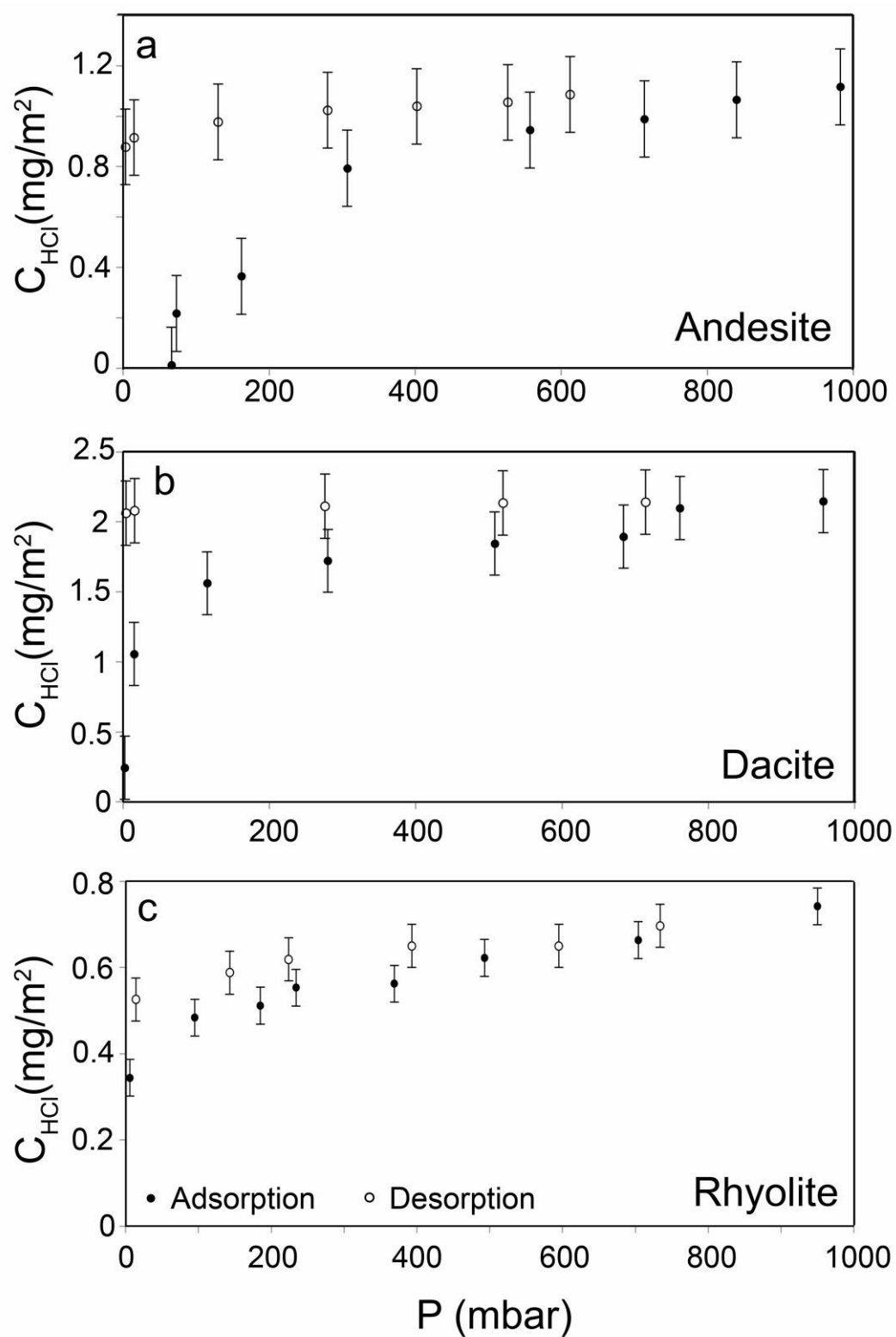


Fig. 2. HCl adsorption and desorption isotherms for (a) andesitic, (b) dacitic, and (c) rhyolitic compositions at room temperature. Error bars are one standard deviation.

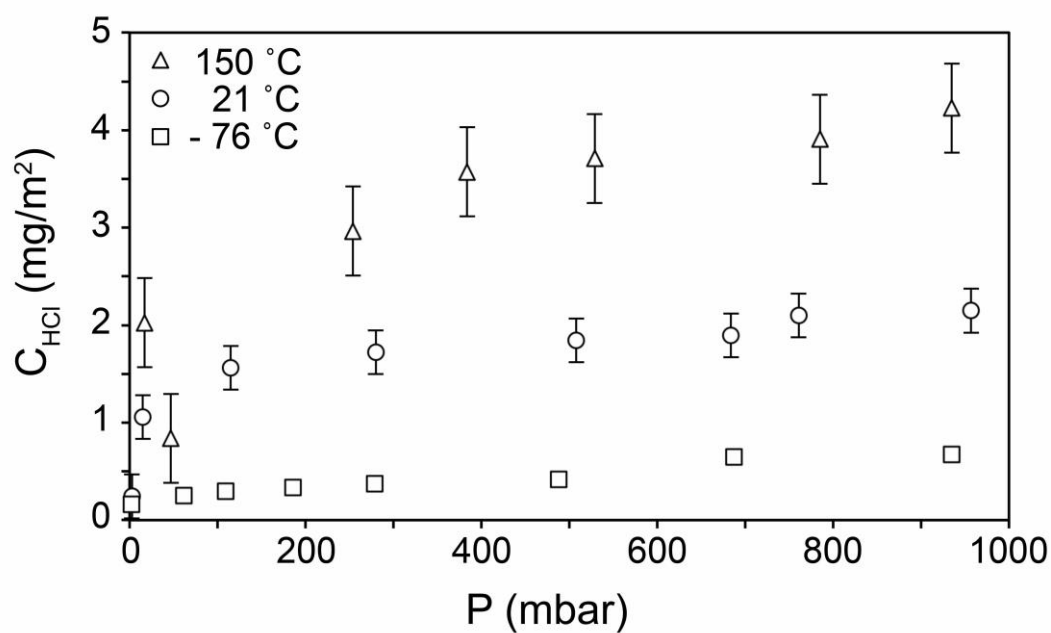


Fig. 3. Effect of temperature on the adsorption of HCl on dacite glass. Error bars are one standard deviation.

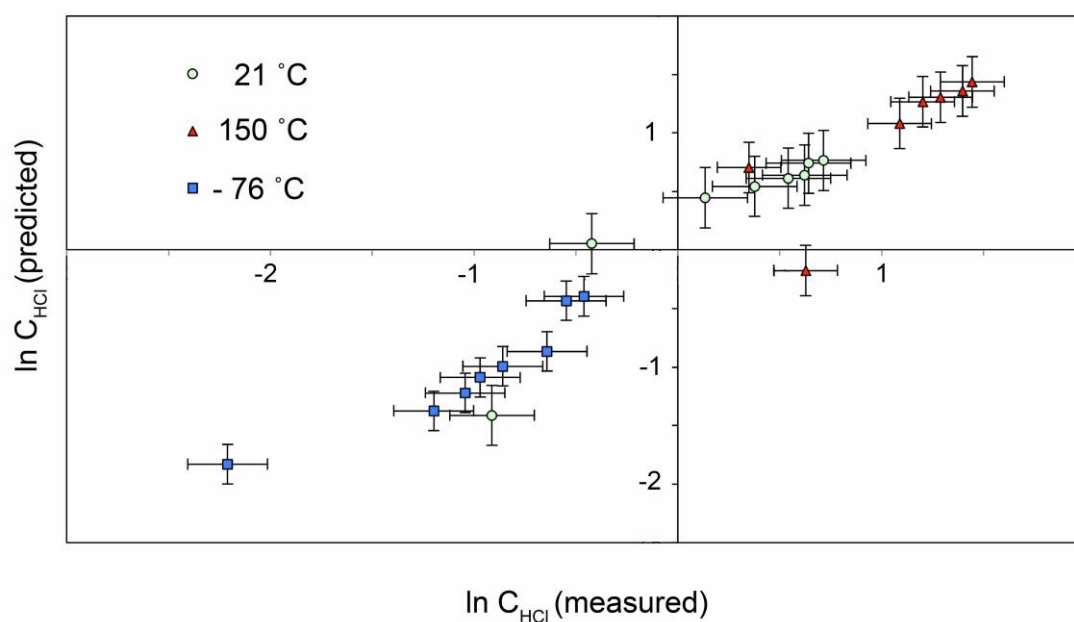


Fig. 4. Multiple regression model for the adsorption of HCl on dacite glass. Surface concentrations c are in mg/m^2 .

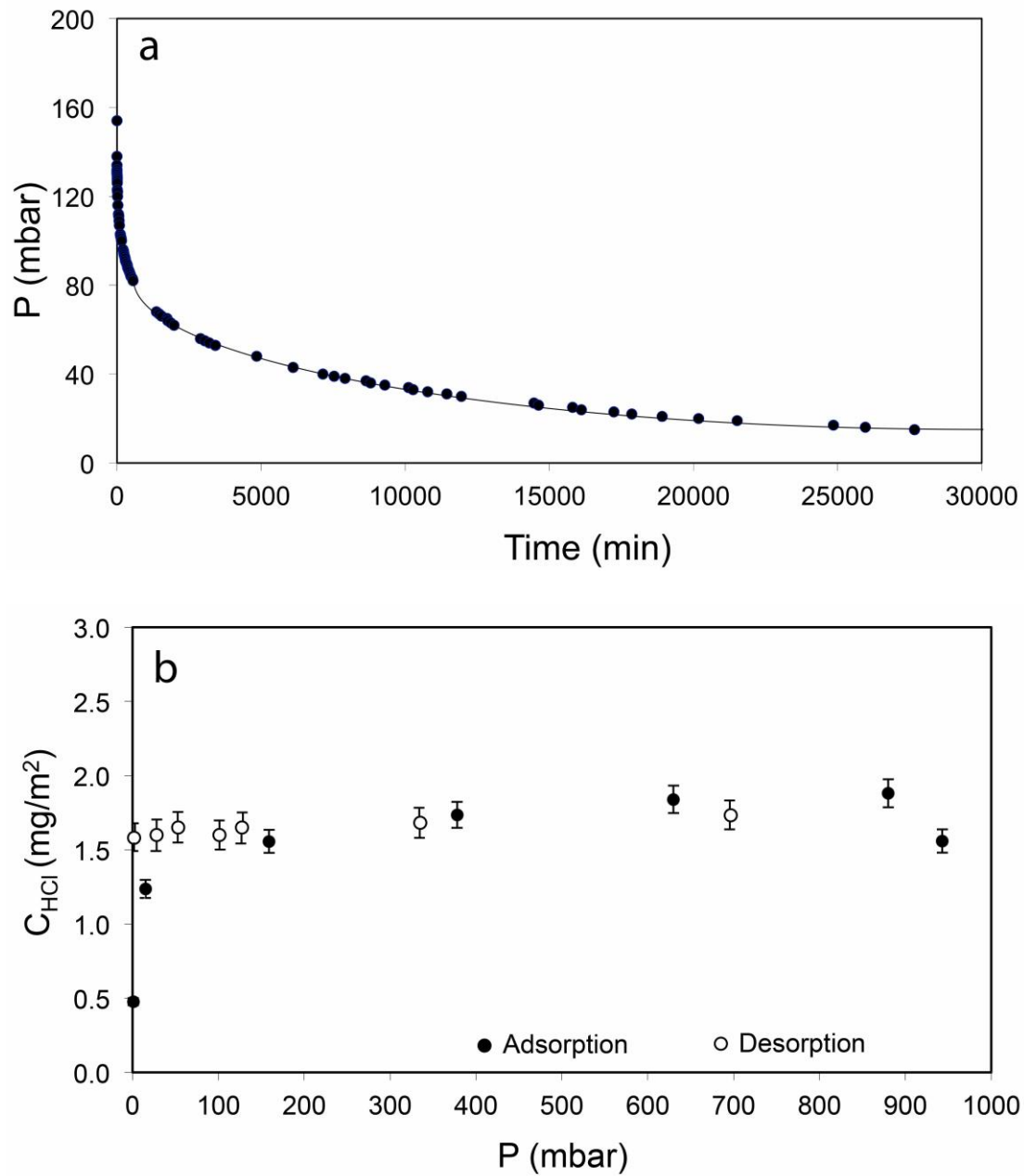


Fig. 5. HCl adsorption on a natural obsidian from the 1739 A.D. eruption of Vulcano (Aeolian Islands, Italy). a) Kinetics of adsorption at room temperature for an initial pressure of $p_0 = 138$ mbar. The decrease in pressure can be described by a rate constant of $\lambda = 1.28 \cdot 10^{-5} \text{ s}^{-1}$; b) Adsorption and desorption isotherms at room temperature. Error bars are one standard deviation. The point at the highest pressure may have been affected by some unknown experimental problem.

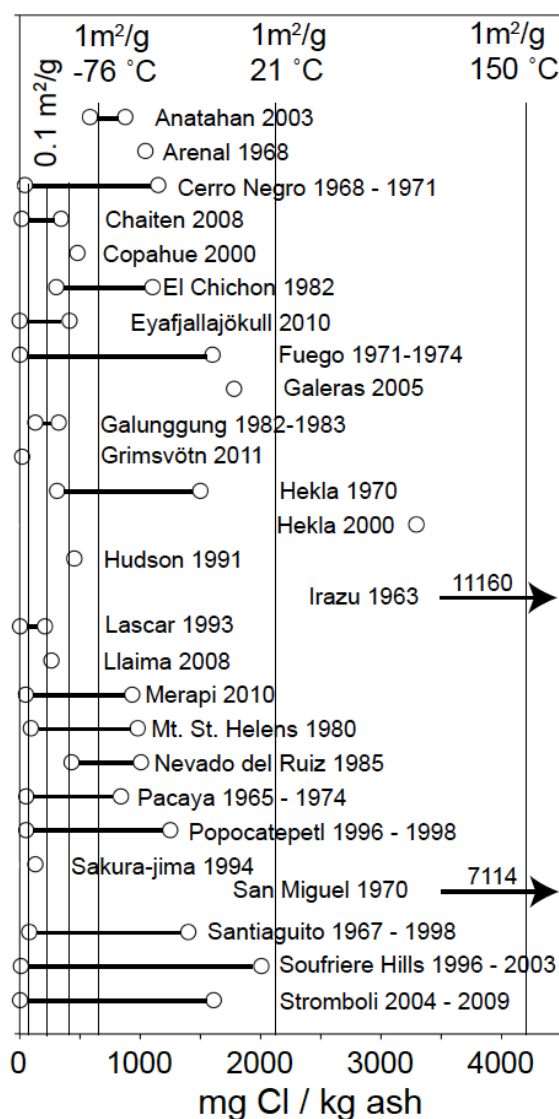


Fig. 6. Concentrations of chlorine adsorbed on volcanic ashes from recent eruptions (see supplementary Table S2 for data and sources). The data are compared with the maximum surface concentrations according to the experimental data for HCl adsorption on dacite glass (vertical lines), assuming two different specific surface areas ($1 \text{ m}^2/\text{g}$ for fine ash, $0.1 \text{ m}^2/\text{g}$ for coarser ash) and adsorption at three different temperatures ($150 \text{ }^\circ\text{C}$, $21 \text{ }^\circ\text{C}$, $-76 \text{ }^\circ\text{C}$). Note that some samples may contain a contribution of Cl-bearing alteration products from other sources, e.g., evaporites, marine aerosols or pre-eruptive interaction with saline groundwaters, altered dome rocks or recycled volcanic ejecta.

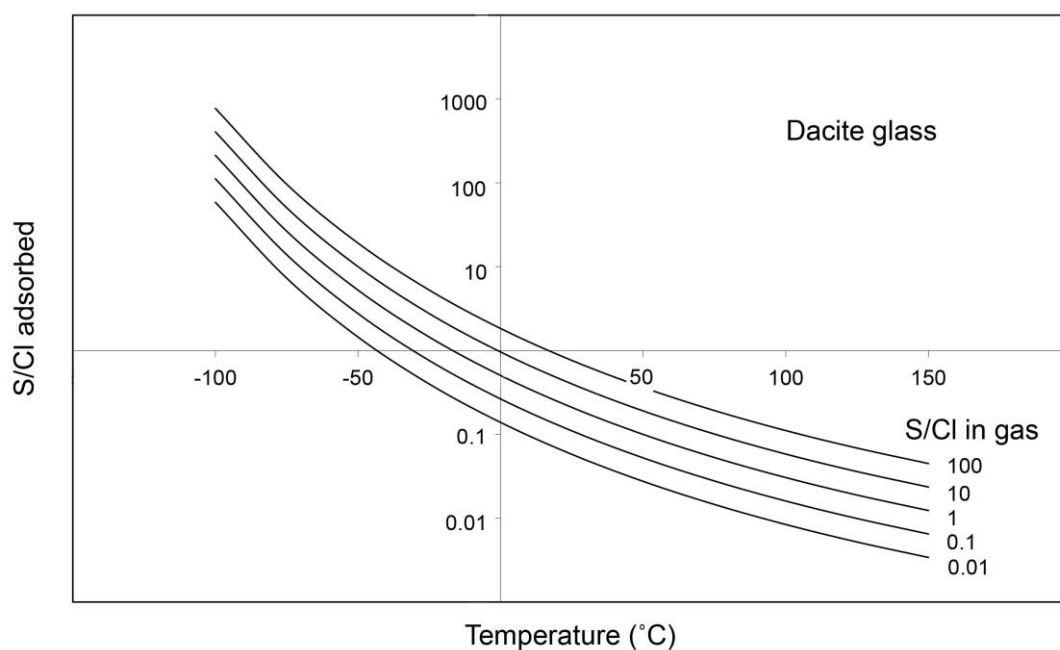


Fig. 7. Calculated fractionation of SO_2 and HCl between volcanic gas and the surface of dacitic ash as a function of temperature.

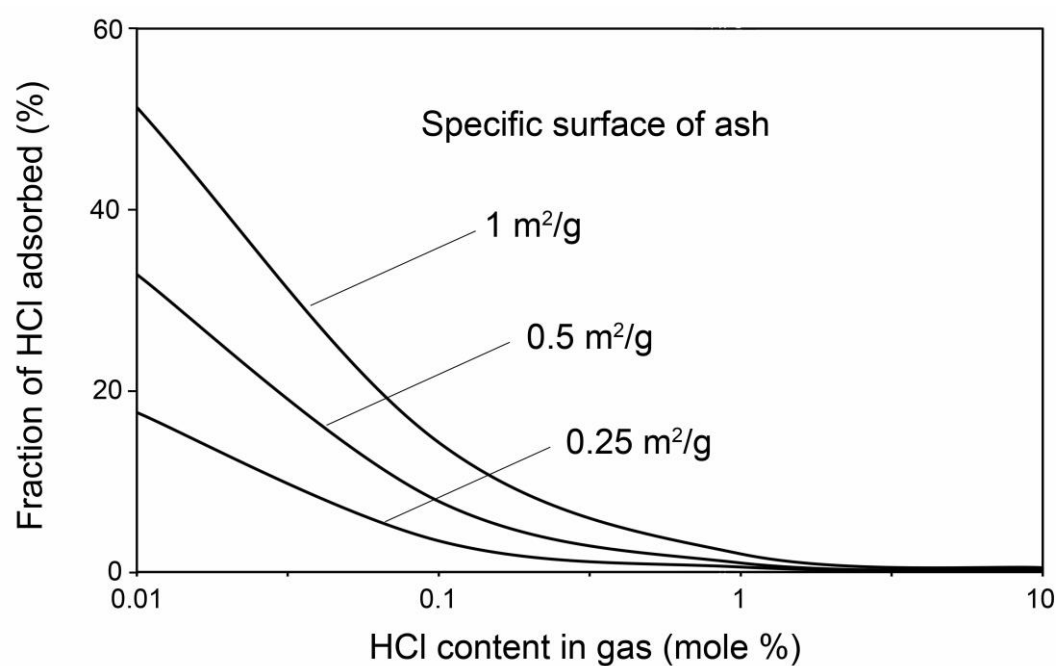


Fig. 8. Fraction of HCl adsorbed on volcanic ash in the umbrella part of a stratospheric plume as a function of initial HCl concentration in the volcanic gas.

Assumptions: Plume altitude 20 km, temperature 220 K, dilution factor 200.